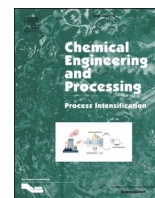




Contents lists available at ScienceDirect

Chemical Engineering and Processing - Process Intensification

journal homepage: www.elsevier.com/locate/cep

Continuous separation and purification of glycerol distillation residues in the sense of circular economy: Experimental proof-of-concept and techno-economic assessment

Maximilian Neubauer, Maximilian Steiner, Max Vogl, Georg Rudelstorfer, Thomas Wallek, Susanne Lux*

Graz University of Technology, Institute of Chemical Engineering and Environmental Technology, NAWI Graz, Inffeldgasse 25C, Graz, Austria

ARTICLE INFO

Keywords:

Glycerol purification
Residue
Sodium chloride
Solid-liquid extraction
Multiphase flow
Process simulation

ABSTRACT

The residue obtained in the course of the distillative purification of crude glycerol from biodiesel production contains mainly inorganic salts like sodium chloride and potassium sulphate, glycerol and matter-organic-non-glycerol. This residue is often discarded, since organic matter is present in the salts which prohibits further use where higher salt purities are needed. However, separation and purification of the residue is of interest, from an environmental but also economic point of view. Here, we demonstrate an experimental proof-of-concept for the separation and purification of glycerol-salt mixtures with ethanol as solvent in continuous counter-current solid-liquid operation in a stirred extraction column, the Taylor-Couette disc contactor. The Taylor-Couette disc contactor proves to be a viable apparatus for this application, especially in view of its simple and robust design with absence of static internals, which limits fouling and prevents accumulation of solids. Furthermore, a techno-economic assessment of the process based on a simulation in AspenPlus was conducted. Economics were evaluated on the basis of capital and operating expenditures, also taking into account waste disposal costs and profits from the sale of value-added products such as purified salt.

1. Introduction

The last two decades have seen a steady rise in biodiesel production worldwide. The annual global production capacity is expected to grow to over 50 billion litres by the year 2026 [1]. In the course of biodiesel production, glycerol arises as by-product, in the magnitude of about 100 kg per ton of biodiesel produced [2]. These amounts of glycerol are exceeding global demands and have led to a decrease in price, making it interesting as a raw material for the production of value-added materials [3–5]. However, for use as feedstock in such processes the crude glycerol from biodiesel production that contains significant amounts of impurities has to be purified in advance [2,6]. Likewise, if the glycerol is to be used in other sectors such as pharmaceuticals or food industry, purification is necessary. Glycerol purification on a commercial scale is usually realized by means of vacuum distillation. In the case of crude glycerol originating from biodiesel production, scraped-wall evaporators are commonly used, due to the high salt content in the crude glycerol (2–5 wt%) [2,7]. The arising distillation residue consists of inorganic salts (sodium chloride and potassium sulphate being the most

common), glycerol and matter-organic-non-glycerol (MONG) such as free fatty acids. The composition varies depending on process setup, process conditions and crude glycerol quality and source. Yong et al. analysed 12 different samples of distillation residue from a palm kernel oil methyl ester plant, with the composition range being as follows: glycerol 8.0–36.3 wt% (mean 20.2 wt%), MONG 4.6–17.7 wt% (mean 12.4 wt%), moisture 0.5–11.2 wt% (mean 3.0 wt%), ash (mainly inorganic salts such as sodium chloride) 57.9–75.5 wt% (mean 64.3 wt%) [8]. The high moisture content of some samples was explained by the hygroscopic nature of the residue in combination with storage in unsealed containers and subsequent absorption of moisture. Immediately after discharge from the bottom of the vacuum distillation column at 190 °C the residue is dry and should stay in that condition if stored in appropriate containers [8].

Up to now, this residue is often deposited in landfills or stored in underground disposal sites [8,9]. However, the high salt content of the residue raises interest for its recovery and utilization as mineral salt for different applications in the sense of circular economy. Furthermore, disposal of waste creates costs for companies, which could be avoided by adding value to such waste streams resulting in net savings and

* Corresponding author.

E-mail address: susanne.lux@tugraz.at (S. Lux).

<https://doi.org/10.1016/j.cep.2023.109465>

Received 15 December 2022; Received in revised form 14 April 2023; Accepted 15 June 2023

Available online 18 June 2023

0255-2701/© 2023 The Authors. Published by Elsevier B.V. This is an open access article under the CC BY license (<http://creativecommons.org/licenses/by/4.0/>).

Nomenclature		C_{TCI}	Total capital investment
<i>Abbreviations</i>		ROI	Return on investment
MONG	Matter-organic-non-glycerol	PBP	Payback period
TCDC	Taylor-Couette disc contactor	<i>Variables</i>	
RDC	Rotating disc contactor	m	Mass [kg]
TCR	Taylor-Couette reactor	\dot{m}	Mass flow [kg/h]
NRTL	Non-Random-Two-Liquid	B	Residue loading [kg/m ² h]
OPEX	Operating expenditures	A	Area [m ²]
CAPEX	Capital expenditures	k	Heat transfer coefficient [kW/m ² K]
LP	Low-pressure	dT	Temperature differential [K]
HP	High-pressure	H	Height [m]
FOB	Free-on-board	D	Diameter [m]
C_{TDC}	Total depreciable capital	HD_{Ratio}	Height to diameter ratio [-]

Table 1
Chemicals used for the batch solid-liquid extraction experiments.

Compound	Supplier	Purity [wt%]	CAS number
Sodium chloride	Roth	≥ 99.8	7647-14-5
Glycerol	Roth	≥ 99.5	56-81-5
Ethanol	Honeywell	≥ 99.8	64-17-5

increasing the economic profitability of processes.

Few literature exists regarding the dedicated separation and purification of this waste stream. Demaman Oro et al. studied the purification of glycerol distillation residue by means of solid-liquid extraction [9]. Different solvents (methanol, ethanol, chloroform, dichloromethane) were evaluated with regard to their effectiveness in extracting organic components from the residue with the goal to obtain purified sodium chloride for further use as mineral salt. The investigated parameters were the solvent to salt ratio and the mixing time. Methanol was found to have the best extraction performance. The quality and recovery of the purified salt were influenced by the solvent to salt ratio, with no significant impact of the mixing time on extraction performance observed. Although a process flow diagram for a continuous process was proposed, the study only covered batch experiments. Az Zahra et al. [10] introduced a theoretical circular economy concept for the regeneration of a biodiesel transesterification catalyst from purified salt obtained from the glycerol distillation residue. Based on the solid-liquid extraction step suggested by Demaman Oro et al., the purified salt is subjected to chlor-alkali-electrolysis to give sodium hydroxide, which is then used to produce transesterification catalyst. However, the solid-liquid extraction step was not in focus and thus taken as proposed by Demaman Oro et al., with no further development or refinements attempted. To summarize, this means that an experimentally-proven continuous process including a first economic feasibility estimate is not available until now.

Therefore, the aim of the present paper is to close the knowledge gap by introducing a methodology for a continuous solid-liquid extraction process of glycerol distillation residues in a stirred extraction column, which will be evaluated experimentally and economically. It shall be noted that the principle goal of the solid-liquid extraction in this case is the purification of the salt matrix contained in the residue, in order to enable utilization as high-purity mineral salt.

2. Methodology

This paper is divided into two main sections. First, the experimental section covers an experimental proof-of-concept for the continuous solid-liquid extraction process. Starting from batch experiments, the development is further transferred towards the process implementation in a stirred extraction column, the Taylor-Couette disc contactor

(TCDC).

The second part of this paper will deal with simulation of a proposed continuous process in Aspen Plus, including a techno-economic assessment.

2.1. Experimental

Parts of the experimental methodology utilized were developed in the course of the work of Steiner [11]. For the whole experimental part, a model residue was used in order to simplify the system. The real glycerol distillation residue consists mainly of inorganic salts such as sodium chloride or potassium sulphate and organic substances, often not analysed in detail quantitatively or even qualitatively. Therefore, a simplification was made in order to develop the process at the early stage. For all experiments, a mixture of 50 wt% sodium chloride and 50 wt% glycerol was used, both components in high purity form, where the sodium chloride represents the solid salt and glycerol the residual organics. Sodium chloride was chosen because it is a common salt found in glycerol distillation residues and has already been covered in literature [9,10]. Basing the process development on a high organics content of the residue represented by glycerol makes the whole methodology more robust, even if in the real case the organics content may be lower such as in the work of Demaman Oro et al. (ash content > 77 wt%) [9]. Although Demaman Oro et al. recommended methanol as extraction solvent [9], ethanol was chosen in this study, due to its lower toxicity, but at the same time comparable properties. Glycerol is completely miscible with ethanol [12], while sodium chloride has a very low solubility in ethanol (0.00065 g / 1 g at 25 °C) [13].

2.1.1. Batch experiments

The chemicals used for the batch experiments are listed in Table 1 and were used without further pre-treatment.

The starting material for the batch experiments was prepared by mixing equal amounts (10 g) of glycerol and sodium chloride at room temperature in a beaker, which resulted in a highly viscous suspension, since sodium chloride is only slightly soluble in glycerol (0.0722 g / 1 g at 25 °C) [2]. After addition of a certain volume of ethanol, corresponding to the desired solvent to salt ratio (ml solvent per gram of salt in the feed), and applying a defined mixing time (1 min), the extract was decanted. In order to gain insight on the effect of multi-stage extraction on this model feed, the steps of decanting and solvent addition were repeated accordingly, with the same amount of fresh solvent added at each stage. The remaining salt after the final stage was then dried for 6 h at 115 °C in a drying cabinet to evaporate residual amounts of ethanol. Finally, the dried salt was treated in a muffle oven at 600 °C for 12 h, volatilizing all residual organics, in this case the residual glycerol. For analysis of the refined salt a simple gravimetric method was applied. The purity of the refined salt was determined by dividing the masses after

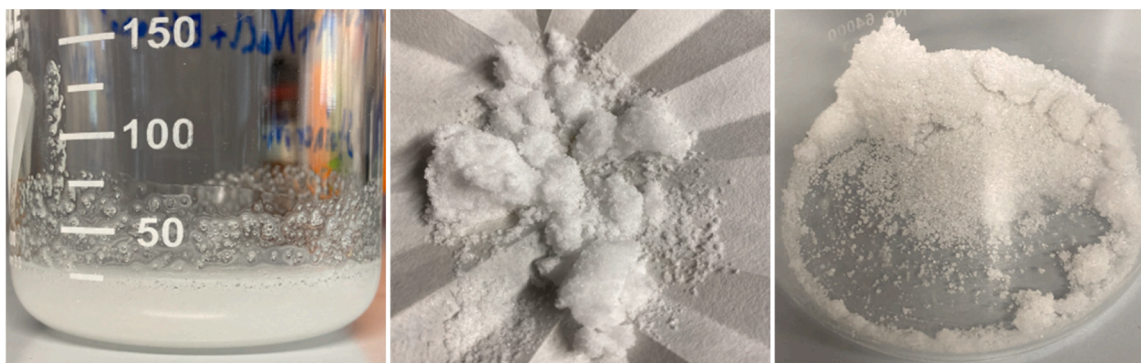


Fig. 1. Left picture: model feed consisting of 50 wt% glycerol and 50 wt% sodium chloride, middle picture: extracted and dried sodium chloride after drying cabinet treatment, right picture: sodium chloride after muffle oven treatment.

Table 2

Chemicals used in the continuous experiments, water content in ethanol determined by Karl-Fischer titration.

Compound	Supplier	Purity [wt%]	CAS number
Sodium chloride	Roth	≥ 99.8	7647-14-5
Glycerol	Roth	≥ 99.5	56-81-5
Ethanol	Brenntag	water content 5.1 wt%	64-17-5
Methyl red sodium salt	Merck	n.a.	845-10-3

and before muffle oven treatment (Eq. (1)).

$$\text{purity}_{\text{NaCl, refined}} [\text{wt}\%] = \frac{m_{\text{NaCl, post muffle}}}{m_{\text{NaCl, pre muffle}}} \cdot 100 \quad (1)$$

The underlying assumption made here is, that all impurities in the refined salt are volatilizable organics, justified by the fact that high purity glycerol and ethanol were used. Fig. 1 shows the steps involved in the experiments.

2.1.2. Continuous experiments

The chemicals used in the continuous experiments are listed in Table 2 and were used without further pre-treatment.

A TCDC was used for the continuous experiments. This apparatus type was developed in the course of research concerning the design simplification of rotating disc contactors (RDC) for multi-stage liquid-liquid extraction [14,15]. The result of this research was a simplified design by abandoning the stator rings, with their task replaced by enlarged rotor disc and shaft diameter. From a hydrodynamic viewpoint, the TCDC is a hybrid between the Taylor-Couette reactor (TCR) and the RDC, which is visualized in Fig. 2.

The stator rings have been abandoned and are replaced with a larger shaft and rotor disc diameter, which avoids any formation of hydraulic dead zones. With this novel design, solids handling in continuous flow becomes possible without accumulation, since no static internals as in the RDC are present and all parts of the apparatus besides the vertical column walls are in constant movement [16,17]. In this work, the TCDC

is the apparatus of choice for two reasons. Firstly, the apparatus has been proven to handle stable solid-liquid flow. Secondly, the principle of extraction columns allows for easy multi-stage operation in counter-current flow, enhancing the efficiency of the process. For more detailed information on the hydraulics and various applications of the TCDC, it shall here be referred to the literature [14–19]. A P&ID of the plant used for continuous solid-liquid extraction experiments is depicted in Fig. 3.

The dimensions of the TCDC used are provided in Table 3, where one compartment refers to the space between two rotor discs.

The feed is conveyed to the column head via pump P1, while solvent enters at the bottom via pump P2. Glycerol is gradually dissolved along the column in ethanol and drawn off at the top into the extract container B3. In further consequence, the solvent ethanol is evaporated from the extract and can be recycled, resulting in the final organic residue consisting of glycerol and traces of sodium chloride. Sodium chloride, which is hardly soluble in ethanol (0.00065 g / 1 g) [13], sediments downwards along the column while being dispersed constantly in a controlled manner and is finally collected in salt sedimentation vessel B4, where it is drawn off after the experiment for further drying steps. The rotational speed of the rotor shaft is controlled and permanently monitored by a computer connected to the stirrer mounted at the top.

Two main process parameters concerning the operation of the TCDC were investigated. First, the minimum rotational speed needed for a stable flow regime and sufficient dispersion of the salt particles inside the compartments was determined by fixing the feed and solvent flow rate and increasing the rotational speed incrementally. The second parameter of interest is the solvent to feed ratio for the solid-liquid extraction process. Here a simple visual approach was taken by colouring the feed with methyl red to achieve a distinctive orange colour in order to visualize the glycerol concentration gradient inside the column. The feed flowrate was fixed and the solvent flowrate was varied in order to achieve a stable colour gradient inside the column. In order to exclude glycerol at the column bottom and to prove the effectiveness of the solid-liquid extraction process the minimum solvent flowrate was defined at the point where the end of the colour gradient was located at the upper

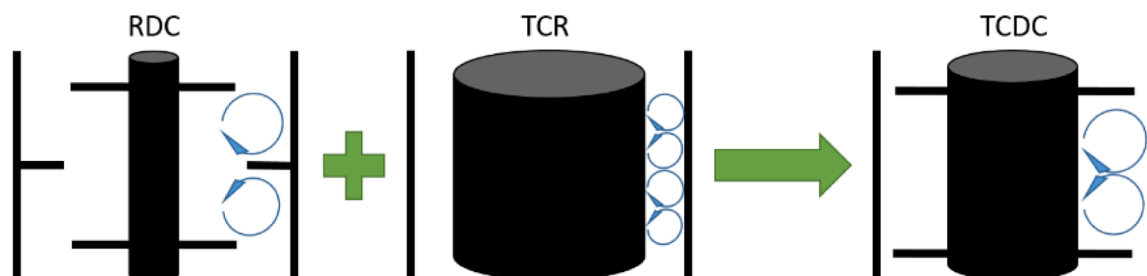


Fig. 2. Hydrodynamic evolution of the TCDC by combination of RDC and TCR characteristics.

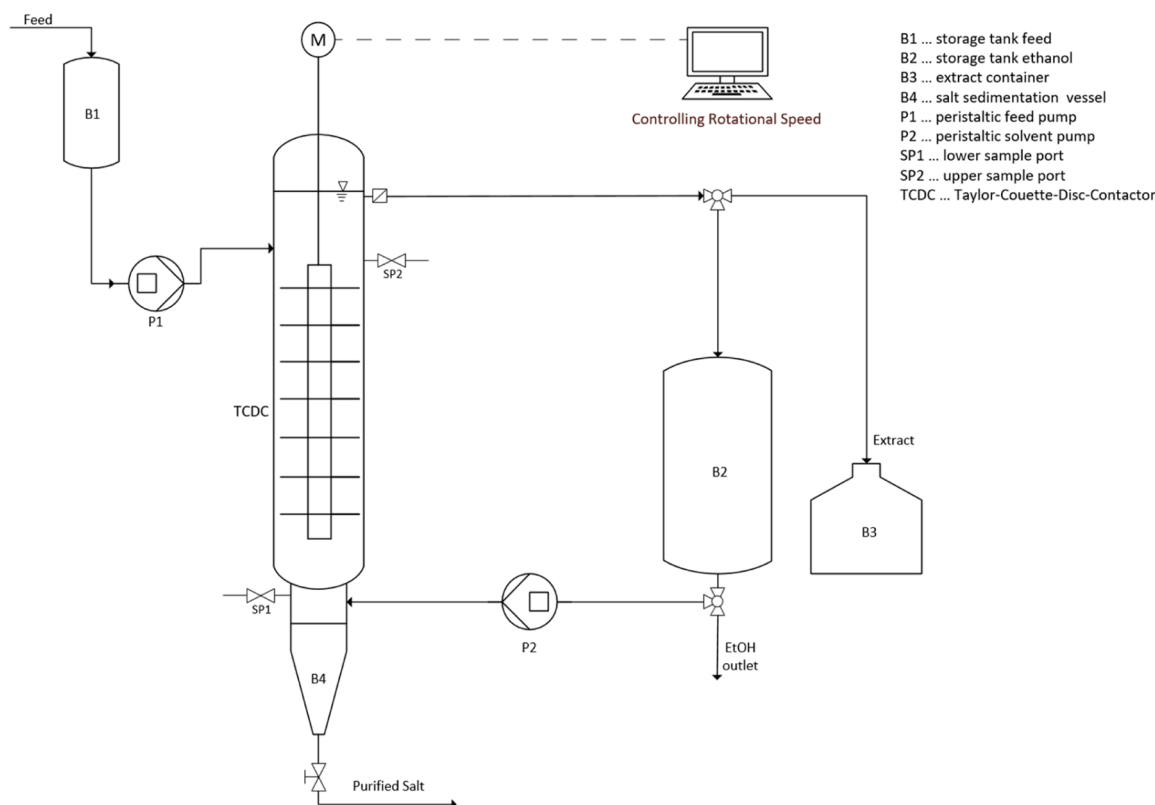


Fig. 3. P&ID of solid-liquid extraction plant.

Table 3

Dimensions and geometry of the TCDC used for the continuous experiments.

Column height [mm]	600
Column diameter [mm]	50
Rotor shaft diameter [mm]	25
Rotor disc diameter [mm]	43
Height of compartment [mm]	25
Number of compartments [-]	24

end of the lower third of the active part of the column. Additionally, liquid samples were taken at sample port SP1 and the mass fraction of glycerol and sodium chloride was determined by evaporating the ethanol at 115 °C in a drying cabinet and subsequently treating the residue in the muffle oven at 600 °C as described in Section 2.1.1.

The purity of the refined salt drawn off at salt sedimentation vessel B4 was determined with the same procedure as in the batch experiments. From the results of these measurements, also the residual moisture of the sedimented salt in vessel B4 was calculated, which was later used in the process simulation as an experimentally determined design variable. Additionally, the recovery of purified salt was calculated by Eq. (2).

$$\text{recovery} [\%] = \frac{m_{\text{refined salt}} \left[\frac{\text{g}}{\text{h}} \right]}{m_{\text{feedstream}} \left[\frac{\text{g}}{\text{h}} \right] \cdot 0.5} \cdot 100 \quad (2)$$

2.2. Process simulation and economic feasibility analysis

2.2.1. Process design

The proposed process for the continuous solid-liquid extraction of the glycerol distillation residue consists of three basic unit operations: solid-liquid extraction, distillation and drying. Starting point is the glycerol distillation residue, which is fed at the top of the TCDC. Recycled solvent enters at the bottom of the column. The refined, wet salt is

drawn off at the bottom of the column and further conveyed into a dryer, where the residual solvent is evaporated and the final dry product is discharged. The solvent is recovered by condensation and recycled back into the process. The extract containing all the organic components is drawn off at the head of the column. In a distillation column, the heavy boiling organics are separated from the solvent, which is again transferred to the closed solvent loop.

2.2.2. Process simulation

The process simulation was set up in AspenPlus V11. In Fig. 4, the flowsheet is depicted.

RESID1 represents the feedstream consisting of 50 wt% glycerol and 50 wt% sodium chloride, with sodium chloride entered as conventional component. Crystallizer SOLU1 adjusts the dissolved amount of sodium chloride according to its solubility in glycerol (0.0722 g NaCl / 1 g at 25 °C) [2], in order to represent the real system where sodium chloride is partly dissolved but mostly present in solid form (RESID2). Solubility of sodium chloride in ethanol (0.00065 g / 1 g at 25 °C) [13] is neglected. The unit operation solid-liquid extraction (TCDC) is simulated by utilizing counter-current-decanter/multi stage solids washer option in Aspen. A solvent stream anhydrous ethanol SOLV enters at the bottom. Three stages with a mixing efficiency of 1 are used, with the liquid to solid mass ratio at the lowest stage set at 0.22 which corresponds to the experimentally determined 18 wt% residual moisture in the wet salt (WETSAL). The wet salt stream WETSAL enters a drying step (DRYER) utilizing low pressure (LP) steam. The model continuous contact dryer was chosen, with the heat transfer coefficient between wall and solids and the wall temperature fixed. Values for these parameters are estimates and taken from literature [20] for a rotary steam tube dryer, listed in the supporting information. The heat transfer area, which is later on needed for equipment cost calculation, was calculated by setting the residual moisture content in the dry product (DRYSAL) as design specification. Solvent vapours from the drying step are condensed in SOLVCOND at atmospheric pressure and recycled back. The extract EXTR

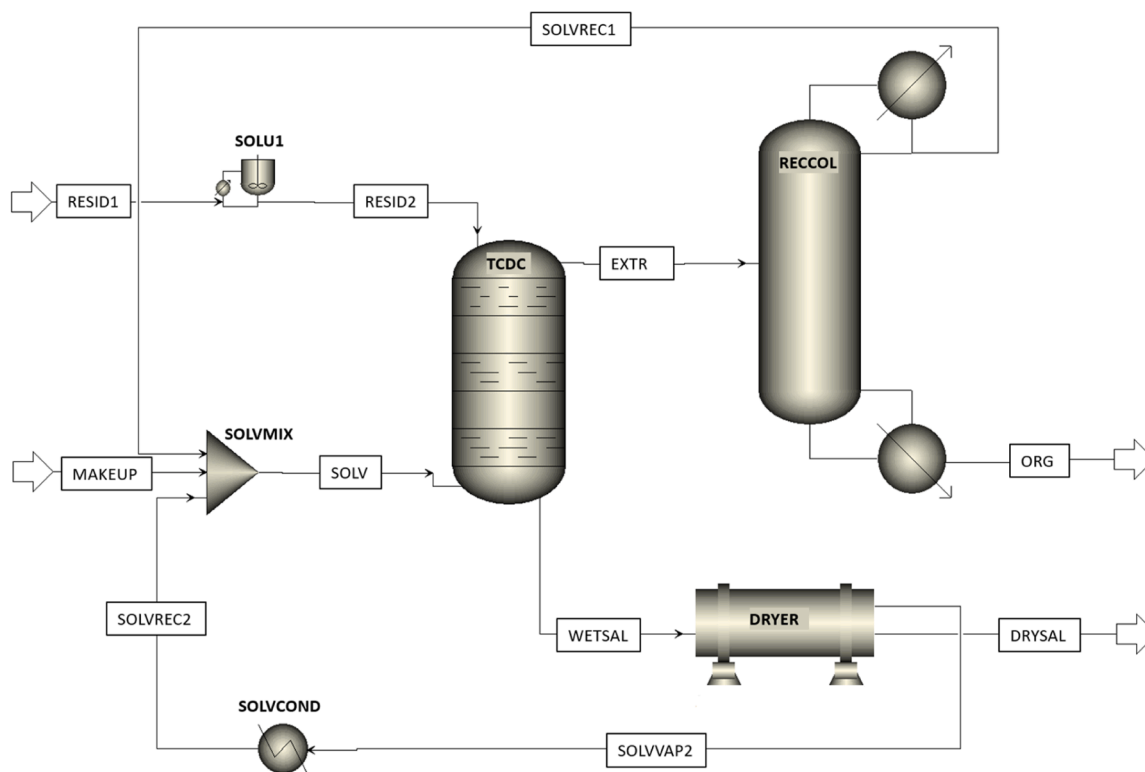


Fig. 4. AspenPlus simulation flowsheet of the proposed solid-liquid extraction plant.

Table 4

Utility costs used for the techno-economic assessment.

Utility	Cost [US\$/GJ]
Cooling water	0.378 [26]
LP steam (6 bar, 160 °C)	7.78 [24]
HP steam (42 bar, 254 °C)	9.88 [24]
Electricity	18.72 [26]

Table 5

Waste disposal costs according to different sources, depending on classification.

Waste disposal cost [US\$/ton]	Reference
36 (non hazardous)	[26]
66 (non hazardous)	[23]
200 (hazardous)	[26]

Table 6

Results of single-stage batch extraction, each experimental measurement point performed twice, mean values are shown.

Solvent to salt ratio [ml:g]	final salt purity [%]
4	97.26
7	98.34
10	98.62

drawn off at the top of the TCDC is separated into solvent recycle SOLVREC1 and organics ORG in solvent recovery column RECCOL. The column is set to operate at 0.15 atm, with 10 equilibrium stages, a total condenser and high pressure (HP) steam used in the reboiler. The residual solvent mass fraction (0.1 wt%) in bottom stream is used as design specification, with the bottoms to feed ratio as adjusted variable. Vacuum operation is chosen because glycerol starts decomposing at its

Table 7

Results of cross flow batch extraction, each experimental measurement point performed twice, mean values are shown.

stage number n	final salt purity after n stages [%]
1	97.26
2	99.74
3	99.96
4	99.97

atmospheric boiling point at 290 °C [21] which would significantly increase fouling, especially in the reboiler section. Still, 0.15 atm allow the use of cheap cooling water (assumed available at 25 °C) in the column head with a distillate temperature of 37 °C. Since the system sodium chloride–ethanol–glycerol does not exhibit a salt effect [22], electrolyte effects are not considered in this simulation. The standard non-random-two-liquid (NRTL) model was chosen to depict the involved vapour-liquid equilibria, with Aspen default parameters used. Ideal behavior of the vapour phase was assumed. The parameters are listed in the supporting information.

2.2.3. Techno-economic assessment

The techno-economic assessment was based on a simplified capital/operating expenditures (CAPEX/OPEX) analysis, including waste disposal cost savings and profits from selling value-added products such as refined salt. For economic evaluation, return on investment (ROI) as well as payback period (PBP) were calculated. For estimation of CAPEX, only major pieces of equipment such as heat exchangers, columns and the dryer were considered, excluding valves and pumps for instance. The only pump considered was a liquid-ring pump for the vacuum system of the solvent recovery column. The liquid-ring pump was chosen according to a heuristic by Seider [23]. These assumptions are considered adequate at this point of process development [24]. Equipment sizing for the dryer and the solvent recovery column was done in Aspen. Heat exchanger sizing was conducted according to Luyben [24]. Sizing of the

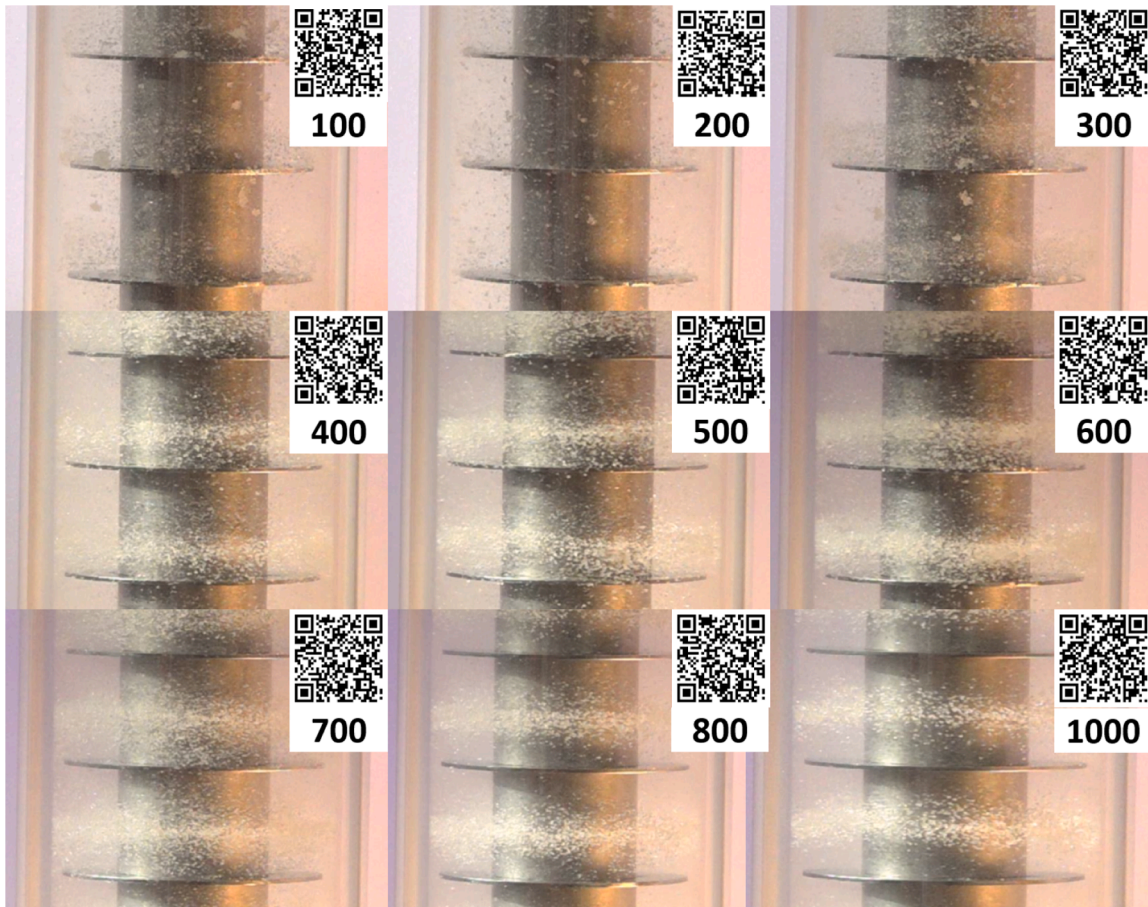


Fig. 5. System sodium chloride – glycerol – ethanol: Snapshots of slow motion videos recorded at different rotational speeds.

liquid-ring pump was done according to Seider [23]. The sizing and scale up of the TCDC was based on laboratory trials with the residue loading as scale up parameter. The residue loading B , which corresponds to a hydraulic column capacity, was calculated by dividing the feed mass throughput by the free cross sectional area (A_{fcs}) of the TCDC (Eq. (3)).

$$B \left[\frac{\text{kg}}{\text{m}^2 \text{h}} \right] = \frac{\dot{m}_{\text{feed,lab}} \left[\frac{\text{kg}}{\text{h}} \right]}{A_{fcs,lab} \left[\text{m}^2 \right]} \quad (3)$$

With a given mass throughput for the scaled up plant, the necessary cross sectional area and consequently the column diameter (D) as well as the column height (H) of the scaled-up column can be calculated Eq. (4), ((5) and (6)) since the height to diameter ratio (HD_{ratio}) is also known from the laboratory column.

$$A_{fcs,scaled} \left[\text{m}^2 \right] = \frac{\dot{m}_{\text{feed,scaled}} \left[\frac{\text{kg}}{\text{h}} \right]}{B \left[\frac{\text{kg}}{\text{m}^2 \text{h}} \right]} \quad (4)$$

$$D \left[\text{m} \right] = 2 \cdot \sqrt{\frac{A_{fcs,scaled} \left[\text{m}^2 \right]}{0.75\pi}} \quad (5)$$

$$H \left[\text{m} \right] = D \left[\text{m} \right] \cdot HD_{ratio} \quad (6)$$

CAPEX equipment correlations were taken from Woods [25]. As a flexible starting basis, the bare module (BM) cost method was applied. It can be adjusted as needed to account for scenario-specific factors to obtain the total depreciable capital (C_{TDC}). To obtain the BM cost, the free-on-board (FOB) equipment costs are multiplied by factors that take into account all costs for concrete, electrical, painting, plumbing, insulation and supports required at a distance of approximately 1 metre from the sides of the equipment unit [25]. Starting from the FOB equipment

cost which is obtained from correlations, the cost for labour and material (LM^*) as well as instrumentation and control systems (IC) is taken into account to give the labour and material cost (LM) according to Eq. (7).

$$LM = [FOB \cdot LM^*] + IC \quad (7)$$

To the LM cost, the FOB cost multiplied by a physical module factor accounting for taxes, freight and insurance (F_{PM}) is added to get the physical module cost PM .

$$PM = LM + [FOB \cdot F_{PM}] \quad (8)$$

The bare module cost (BM) is obtained by adding the LM cost multiplied by a bare module factor accounting for offsites, indirects for home office and field expenses (F_{BM}) to the PM cost.

$$BM = PM + [LM \cdot F_{BM}] \quad (9)$$

The total bare module cost is calculated by summation of the BM cost for the major pieces of equipment.

$$BM_{total} = \sum BM_{unit} \quad (10)$$

The C_{TDC} is obtained by multiplying the total bare module cost by factors (F_{TDC}) taking into account contingencies for unexpected delays and changes in scope during construction as well as contractor fees.

$$C_{TDC} = BM_{total} \cdot (1 + F_{TDC}) \quad (11)$$

For calculation of ROI and PBP, further the total capital investment (C_{TCI}) is needed, which is calculated from the C_{TDC} by taking into account land, working capital and startup expenses (F_{TCI}).

$$C_{TCI} = C_{TDC} \cdot (1 + F_{TCI}) \quad (12)$$

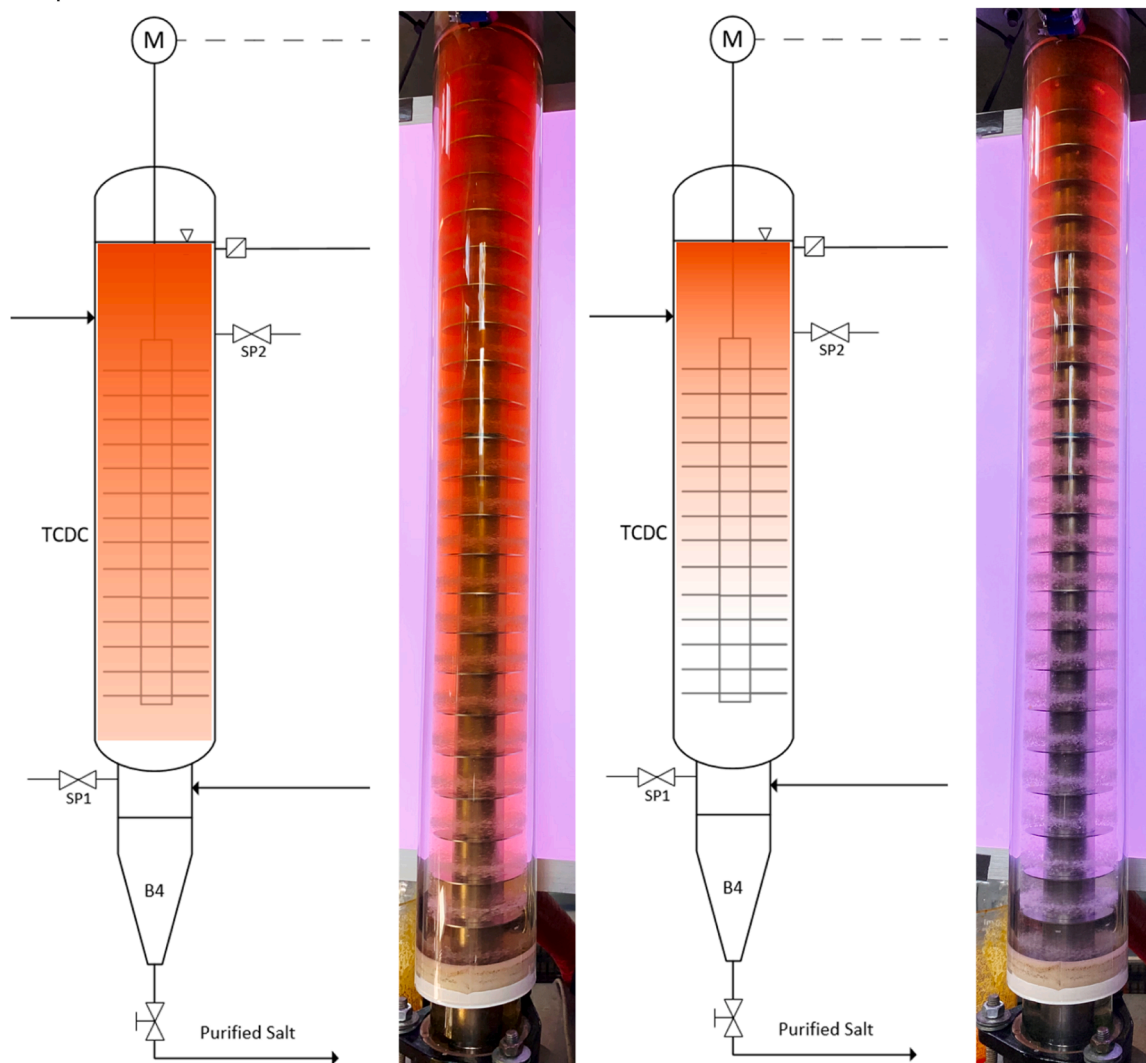


Fig. 6. Visualization of the methodology to evaluate the minimum solvent flowrate, left side: insufficient solvent flowrate, right side: sufficient solvent flowrate.



Fig. 7. Intermediate and final products of the experimentally evaluated process in continuous mode, 1) feed, 2) wet, refined salt, 3) extract, 4) dried refined salt, 5) recycled solvent, 6) organic residue (glycerol), colouring agent: methyl red.

Finally the *ROI* and *PBP* are calculated according to Eqs. (13) and (14) from Seider [23], where *t* stands for the taxation rate, *S* for the annual revenues considering profits from selling purified salt and savings by elimination of waste disposal costs, *C* for the annual production

costs and *D* for the annual depreciation.

$$ROI = \frac{(1 - t)(S - C)}{C_{TCI}} \tag{13}$$

Table 8

Experimental process summary, results from continuous experiments, mean values from triplicate sample analysis shown.

	Solvent fraction extract [wt %]	Glycerol fraction extract [wt %]	Salt fraction extract [wt %]	Recovery salt [%]	Salt purity final [%]
Solvent to salt ratio 4.3: 1	76.6	22.2	1.2	94.6	99.88
Solvent to salt ratio 9.7: 1	88.0	11.4	0.6	94.5	99.94

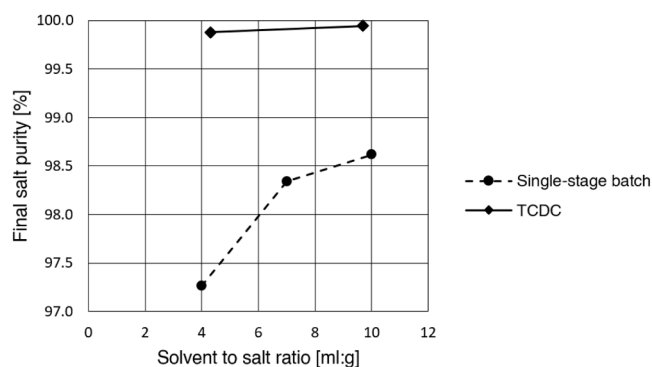


Fig. 8. Results of single-stage batch extraction compared to continuous counter-current operation in the TCDC.

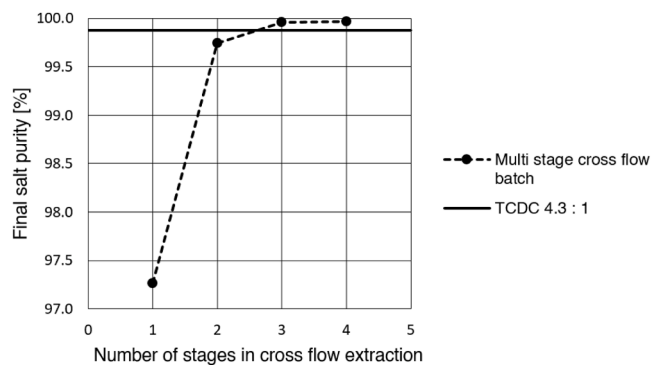


Fig. 9. Results of multi-stage cross flow batch extraction (solvent to salt ratio 4 : 1 for each stage) compared to continuous counter-current operation in the TCDC (solvent to salt ratio 4.3 : 1).

$$PBP = \frac{C_{TDC}}{(1-t)(S-C) + D} \quad (14)$$

Utility costs for calculating OPEX are listed in Table 4.

Different waste disposal cost scenarios were considered and are listed in Table 5 below.

The hazardous classification was included in the assessment, since the residue may very well be classified as hazardous waste in some countries, for instance the United States [27], due to its high alkalinity [8,28].

For calculating profits from selling value-added products, the quality of the refined salt from the solid-liquid extraction process is assumed to be comparable with solar salt. The price per ton of solar salt was averaged over the time period from 2017 to 2021 [29], amounting to 120 US \$/t.

All correlations, cost factors and calculation details are listed in the supporting information.

3. Results and discussion

3.1. Batch experiments

The experiments were conducted according to the methodology described in Section 2.1.1. In Table 6, the results of single-stage batch extraction at three different solvent to salt ratios are shown.

As can be seen, single-stage extraction even at high solvent to salt ratios fails to achieve high salt purities $\geq 99.8\%$, which is set as desirable specification for use in various industrial applications. This points towards multi-stage operation being more economic in regard to solvent demand. Results of cross flow batch extraction are shown in Table 7. For each stage, 40 ml of fresh solvent were used.

To achieve purities $\geq 99.8\%$, at least three stages in cross flow extraction are needed. Furthermore, it has to be considered that in this experiment, a model feed consisting of high purity sodium chloride and glycerol was used. It has to be taken into account that in the real residue, organics will be incorporated inside the salt crystals, which form during evaporation/distillation. Additionally, organic components with lower solubility in polar solvents such as long-chain fatty acids may be present. All these considerations result in a working hypothesis in which multi-stage extraction is considered as the safest and most robust option for residue purification.

3.2. Continuous experiments

3.2.1. Rotational speed

The feed flowrate for investigating the influence of different rotational speeds was 2 kg/h, with a solvent flow rate of 5 l/h. The feed used consisted of 50 wt% sodium chloride and 50 wt% glycerol. Starting from 100 rotations per minute (rpm) the speed was incrementally increased by steps of 100 rpm. Fig. 5 shows the results of this investigation. The pictures are snapshots taken from videos recorded by a slow motion camera (can be accessed by the QR-codes in Fig. 5 or via link in the supporting information), with two compartments located in the middle of the column in focus.

Having a closer look at the pictures in Fig. 5 but more so the slow motion videos, it can be concluded that the minimum rotational speed lies in the range between 400 and 500 rpm. Below, energy input is not sufficient and particle agglomerates sediment downwards without being dispersed resulting in decreased mass transfer. With higher rotational speeds, also the strength of the Taylor vortices inside the compartments increases, leading to the formation of a distinct ring-shaped accumulation of particles at the shear interface of the two counter-rotating Taylor vortices in the middle of the compartment. For all subsequent experiments, a rotational speed of 600 rpm was chosen since sufficient dispersion is ensured while at the same time the benefit from rotational speeds above 600 rpm is limited.

3.2.2. Minimum amount of solvent

As described in Section 2.1.1, a visual methodology was developed for determining the minimum amount of solvent needed in order to exclude the presence of glycerol at the lower end of the column. Again the feed used was a mixture of 50 wt% glycerol and 50 wt% sodium chloride, coloured with 0.02 wt% methyl red. The feed flowrate was fixed at 1.8 kg/h and the solvent flowrate was varied incrementally. After each change of the solvent flowrate, the shift of the colour gradient was monitored until stationary operation, represented by a static gradient. After keeping the gradient at these points for 7 min, a new solvent flowrate was set. The minimum amount of solvent was defined at the point, where the end of the colour gradient was located at the upper end of the lower third of the active part of the column. This methodology is depicted in Fig. 6, with an insufficient solvent flowrate shown on the

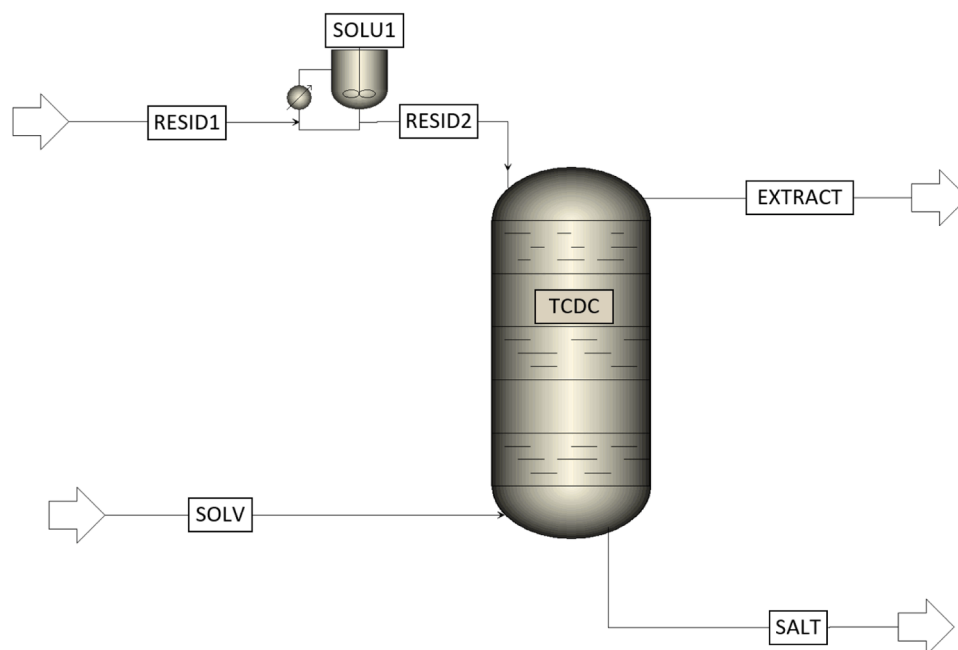


Fig. 10. Simulation setup used for model validation, counter-current-decanter (CCD) including inlet and outlet streams.

left side, where the colour gradient extends well below the lower end of the active part of the column. On the right side, the solvent flowrate is sufficient to exclude glycerol in the lower compartments.

The result of these conceptual trials is that below a solvent to salt ratio of 4:1, glycerol presence cannot be excluded at the lower end of the column. Therefore, a solvent to salt ratio of 4:1 is considered as the necessary minimum. Gravimetrically analysed samples taken from sampling point SP1 confirmed the applied methodology as the mass fraction of glycerol in the solvent phase was below 0.001 at a solvent to salt ratio of 4:1.

3.2.3. Experimental process summary

Fig. 7 gives an overview of intermediate and final products of the experimentally evaluated process in continuous mode.

The residue, in this case represented by a mixture of 50 wt% sodium chloride and 50 wt% glycerol, is purified by counter-current solid-liquid extraction in a TCDC. Glycerol is gradually dissolved along the column in the solvent ethanol and transported upwards forming the extract. Sodium chloride does not dissolve in significant amounts in ethanol and sediments downwards while being constantly dispersed. Still, due to the presence of glycerol in the extract and the higher solubility of sodium chloride therein, sodium chloride is also found in the extract. The use of anhydrous ethanol as solvent would decrease the sodium chloride content in the extract. The technical grade ethanol used in these trials contains significant amounts of water (5.1 wt%), which exhibits a much higher solubility of sodium chloride (0.359 g / 1 g at 20 °C) [13] than ethanol (0.00065 g / 1 g at 25 °C) [13]. The residual moisture of the sedimented salt averages 18 wt% solvent, analysed from the experiments shown in Table 6. This value is later on used as design variable in the process simulation. Two experimental operating points, which are later also used for validation of the counter-current-decanter model in Aspen, are shown in Table 8.

This shows that the proposed process is effective for the generation of purified salt with good recovery. A final remark on solvent regeneration shall be made. The large difference in vapour pressures between ethanol/water and glycerol allow for rather simple regeneration, which was performed during the course of the experimental trials in a conventional rotary evaporator. Since ethanol, water and glycerol are substances with well investigated thermodynamics even in combination

with sodium chloride [22], no dedicated experiments were made in regard to solvent recovery. The process simulation results are assumed to be reliable in this regard.

3.3. Comparison between batch and continuous experimental results

Intensification of processes through solvent demand reduction is relevant from an economic point of view. In order to assess the performance of the TCDC, the results from the continuous counter-current experiments are compared to single-stage batch as well as multi-stage cross flow batch experiments. Fig. 8 shows the comparison between single-stage batch experiments and continuous counter-current operation in the TCDC in regard to achievable final salt purity. The numeric values are listed in Tables 6–8.

This shows that the performance of the TCDC is superior to single stage extraction at comparable solvent to salt ratios. Further, the extraction performance of multi-stage cross flow batch and continuous counter-current operation is compared in Fig. 9.

In Fig. 9, it can be seen that the TCDC performs at least as well as two-stage cross flow extraction, while at the same time operating with around half the amount of solvent. This confirms that the chosen apparatus type enables significant reduction of solvent demand and thus also energy costs related to the solvent recovery resulting in an intensified process.

3.4. Model validation

In order to validate the counter-current-decanter model in Aspen, which is used to simulate the TCDC, experimental data is compared to simulation results. Since drying and distillation are considered mature technology, the validation is focused on the counter-current-decanter. Two experimental operating points of the TCDC plant were analysed. With the feed composition (50 wt% glycerol, 50 wt% sodium chloride), the total extract flowrate and extract composition known, all missing flow variables can be determined via a simple mass balance. The simulation only considers the apparatus itself, including inlet and outlet streams, since this corresponds to the experimental setup. The flowsheet is shown in Fig. 10.

In the experiments, the salt from sedimentation vessel B4 (Fig. 3) is

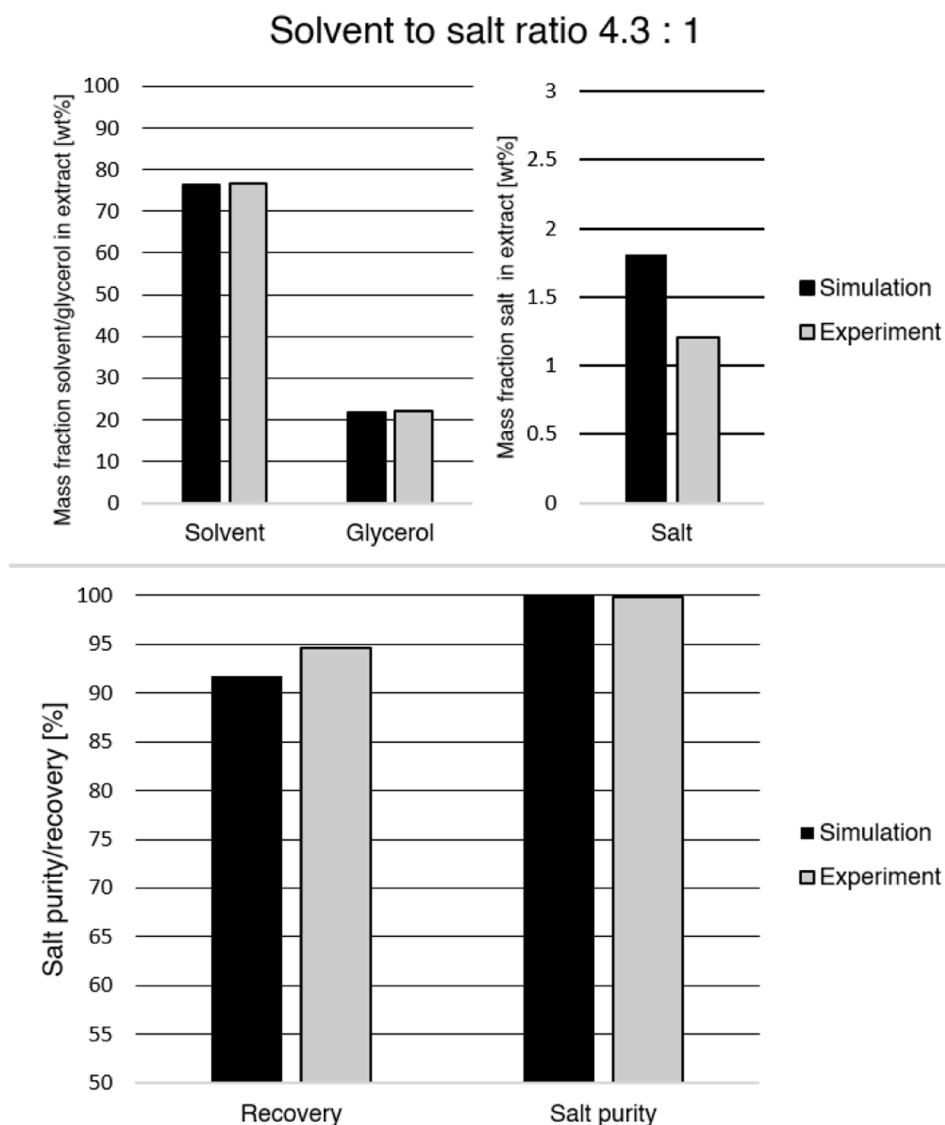


Fig. 11. Comparison of experimental and simulation results for a solvent to salt ratio of 4.3 to 1.

drawn off periodically, as described in the experimental section. Therefore, at a stationary operating point, a continuous stream SALT in the experiments does not exist. In order to simulate the experimental setup nonetheless, the solvent content of the SALT stream is set to zero, with the solvent-free salt leaving the block. This ensures a formally accurate depiction of the experimental operating points. The results of the model validation are shown graphically in Figs. 11 and 12. The numeric experimental values are shown in Table 8.

The validation shows satisfying agreement between experimental and simulation results, especially concerning solvent and glycerol content in the extract. The mass fraction of salt in the extract shows somewhat larger deviations, with the experimental value being lower for both operating points. A likely reason for this observation is that the simulation does not consider mixed-solvent effects, where ethanol decreases the solubility of sodium chloride in glycerol, acting as anti-solvent [30]. As a consequence of lower salt content in the extract for the experimental process compared to the simulation, the recovery of salt in the experiments is also higher. For the techno-economic assessment, no negative impact is expected from this outcome, since over-estimation of process performance is ruled out, with the experiments showing even slightly better results. Finally, both simulation and experimental results confirm a very high achievable salt purity $\geq 99.8\%$.

3.5. Techno-economic assessment

The basis for the assessment was a solid-liquid extraction plant with a capacity of 10 kt residue per year (1142 kg/h), consisting of 50 wt% sodium chloride and 50 wt% glycerol. This corresponds to the waste residue stream of a glycerol purification plant with a capacity of 100 kt/year crude glycerol, assuming a salt content of 5 wt% in the crude glycerol [9,31]. The extraction solvent was anhydrous ethanol, with a solvent to salt ratio of 5:1 (l:kg). The 10 kt/year process was simulated in AspenPlus, an excerpt of the results is shown in Table 9, where the reboiler and condenser duties of major process equipment are listed. The complete heat and material balance is provided in the supporting information.

A summary of C_{TDC} and C_{TCI} as well as OPEX assessment is shown in Table 10. The OPEX amount to 25 US\$/t of residue processed. Calculation details are listed in the supporting information.

As mentioned in Section 2.2.2, ROI and PBP were calculated for different waste disposal scenarios. The results are shown in Fig. 13.

As can be seen in Fig. 13, the ROI as well as the PBP are strongly depending on the waste disposal costs. Concerning the three scenarios, at a waste disposal cost of 36 US\$/t, the economic attractiveness is rather low at a ROI beyond 10%. As the waste disposal cost increases,

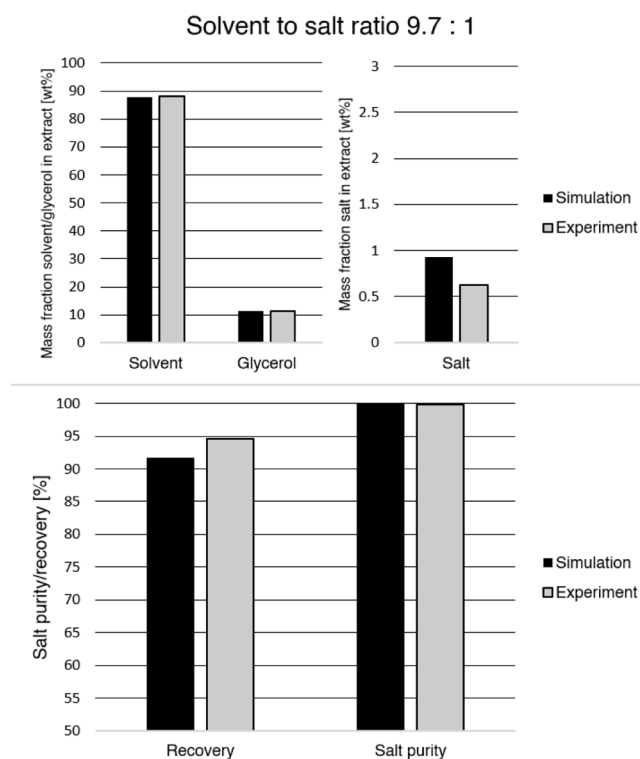


Fig. 12. Comparison of experimental and simulation results for a solvent to salt ratio of 9.7 to 1.

Table 9

Heat duties of major equipment for simulated 10 kt/year plant.

Equipment	Duty [kW]
Reboiler solvent recovery column	728
Condenser solvent recovery column	644
Dryer	50
Condenser dryer	35

Table 10

Results of techno-economic assessment for a 10 kt/year solid-liquid extraction plant; C_{TDC} , C_{TCI} and OPEX.

C_{TDC} [US\$]	2,190,220
C_{TCI} [US\$]	3,329,134
OPEX [US\$/year]	247,497

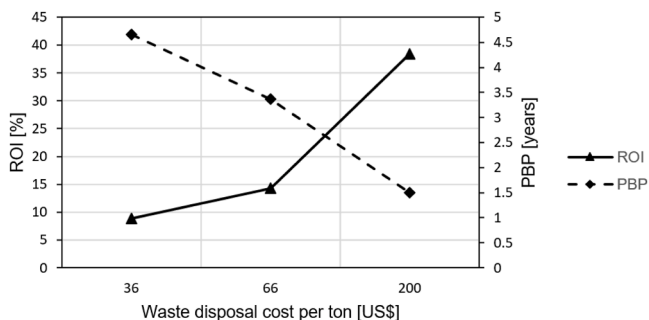


Fig. 13. ROI and PBP as a function of waste disposal costs.

also the ROI increases, and in consequence the PBP decreases. At 66 US \$/ton disposal cost, the ROI is around 15%, with the ROI increasing up to 38% if the residue would be considered as hazardous. The low ROI

values for non-hazardous classified waste were expected, since sodium chloride is not a high value commodity. However, it has to be taken into account that this result represents the lower end of economic profitability. For this study, sodium chloride as inorganic pollutant in crude glycerol was chosen because of industrial relevance, which is also supported by literature available concerning sodium-based residues [8–10]. As mentioned in the introduction section, potassium sulphate is also a common salt found in crude glycerol. At an average trading price of 496 US\$/ton (average 2015–2018 United States [32]), which is around four times higher than the trading price of sodium chloride, the economic profitability is expected to increase extensively. Furthermore, the transferability of the process from sodium chloride to potassium sulphate is expected to proceed without major issues, since both are inorganic alkali salts with low solubility in organic solvents. However further research has to be conducted in this regard in order to confirm and support these assumptions. Another aspect which should be taken into account is the trend of increasing cost of waste disposal and landfill fees in the future [33,34], which will definitely impact considerations of processes like the one outlined in the present paper. At last, the utilization of the organic part of the residue obtained after evaporation of the extract depends on its composition and is not included in the assessment. If the glycerol content is very high, the yield of the crude glycerol purification process can be further improved. In any case, the remaining organics (glycerol, free fatty acids or soaps) are expected to be useable either for generating process heat or as feedstock for biogas production. This would further increase the economic benefit of separating and purifying the glycerol distillation residue waste stream. At least, with a high certainty, no significant additional cost arising from the organic part of the residue is expected.

4. Conclusion

A methodology for the separation and purification of glycerol distillation residues by means of counter-current solid-liquid extraction was presented. First, an experimental proof-of-concept was conducted in a laboratory-scale stirred extraction column. The Taylor-Couette disc contactor was chosen as device for the continuous solid-liquid extraction process, which is very well suited for processes involving solids, due to the absence of static column internals. A model feed consisting of 50 wt % glycerol and 50 wt% sodium chloride was separated and purified by counter-current extraction with ethanol, yielding sodium chloride with a high purity of ≥ 99.8 wt%. Evaluation of process parameters showed that the desired flow regime inside the column starts appearing between 500 and 600 rpm with a minimum solvent to salt ratio of 4:1 (l:kg). The second part of this study was a techno-economic assessment. A process simulation for the continuous counter-current solid-liquid extraction was setup in Aspen Plus, partly based on experimentally determined design variables. Model validation was conducted by comparing experimental data to simulation results, with satisfying agreement observed. The design of the proposed process was held simple, with three main unit operations at the core (solid-liquid extraction, solvent regeneration/distillation and drying). Economics were evaluated on a CAPEX/OPEX basis, as well as taking into account waste disposal costs and profits from selling value-added products such as refined salt. Return on investment and payback period were calculated depending on different waste disposal cost scenarios. With increasing waste disposal costs, the economic profitability of the proposed process increases. Furthermore, the composition of the residue especially in regard to the type of inorganic salt (sodium chloride vs. potassium sulphate) is expected to have a major impact on economics. A follow-up project will deal with further refinement of the proposed process, including the evaluation of different residue compositions, also regarding the type of salt incorporated in the residue, as well as energetic optimization of the proposed process.

Declaration of Competing Interest

The authors declare that they have no known competing financial interests or personal relationships that could have appeared to influence the work reported in this paper.

Data availability

Data will be made available on request.

Acknowledgment

Financial support by the Austrian Research Promotion Agency (FFG) is gratefully acknowledged (FFG project number: 879587).

Supplementary materials

Supplementary material associated with this article can be found, in the online version, at [doi:10.1016/j.cep.2023.109465](https://doi.org/10.1016/j.cep.2023.109465).

References

- [1] International Energy Agency. Renewables 2021 <https://iea.blob.core.windows.net/assets/5ae32253-7409-4f9a-a91d-1493fb9777a/Renewables2021-Analysisandforecastto2026.pdf> (accessed Aug 10, 2022).
- [2] R. Christoph, B. Schmidt, U. Steinberner, W. Dilla, R. Karinen, Glycerol. Ullmann's Encyclopedia of Industrial Chemistry, Wiley-VCH Verlag GmbH & Co. KGaA, Weinheim, Germany, 2006, <https://doi.org/10.1002/14356007.a12.477.pub2>.
- [3] M. Pagliaro, R. Ciriminna, H. Kimura, M. Rossi, C. Della Pina, From glycerol to value-added products, *Angew. Chemie Int Ed* (24) (2007) 4434–4440, <https://doi.org/10.1002/anie.200604694>.
- [4] Dimitratos, N.; Villa, A.; Chan-Thaw, C.E.; Hammond, C.; Prati, L. Valorisation of Glycerol to Fine Chemicals and Fuels; 2016; pp 352–384. <https://doi.org/10.4018/978-1-4666-9975-5.ch013>.
- [5] J. Kaur, A.K. Sarma, M.K. Jha, P. Gera, Valorisation of crude glycerol to value-added products: perspectives of process technology, economics and environmental issues, *Biotechnol. Rep.* 27 (2020) e00487, <https://doi.org/10.1016/j.btre.2020.e00487>.
- [6] F. Yang, M.A. Hanna, R. Sun, Value-added uses for crude glycerol—a byproduct of biodiesel production, *Biotechnol. Biofuel.* 5 (1) (2012) 13, <https://doi.org/10.1186/1754-6834-5-13>.
- [7] Knothe, G.; Van Gerpen, J.; Krahl, J. *The Biodiesel Handbook*; Knothe, G., Van Gerpen, J., Krahl, J., Eds.; AOCS Publishing, 2005. <https://doi.org/10.1201/9781439822357>.
- [8] K.C. Yong, T.L. Ooi, K. Dzulkefly, W.M.Z. Wanyunus, a H Hazimah, Characterization of glycerol residue from a palm kernel oil methyl ester plant, *J. Oil Palm Res.* 13 (2) (2001) 1–6.
- [9] C.E. Demaman Oro, M. Bonato, J.V. Oliveira, M.V. Tres, M.L. Mignoni, R. M Dallago, A new approach for salts removal from crude glycerin coming from industrial biodiesel production unit, *J. Environ. Chem. Eng.* 7 (1) (2019), 102883, <https://doi.org/10.1016/j.jece.2019.102883>.
- [10] Az Zahra, A. Choirun, I. Arina Rusyda, A. Hizbiyati, F. Giovani, N. Zahara, B. Jiwandaru, D. Gunawan, G. Andre Halim, M. Pratiwi, A. Nur Istyami, A. Verani Rouly Sihombing, A. Harimawan, D. Sasongko, J. Rizkiana, Novel approach of biodiesel production waste utilization to support circular economy in biodiesel industry, *IOP Conf. Ser. Mater. Sci. Eng.* 1143 (1) (2021), 012030, <https://doi.org/10.1088/1757-899x/1143/1/012030>.
- [11] M Steiner, Separation and Utilization of Glycerol Purification Byproducts in View of Circular Economy, Graz University of Technology, 2021. MSc Thesis.
- [12] L.R Morrison, Glycerol. Kirk-Othmer Encyclopedia of Chemical Technology, Wiley, 2000, <https://doi.org/10.1002/0471238961.0712250313151818.a01>.
- [13] G. Westphal, G. Kristen, W. Wegener, P. Ambatiello, H. Geyer, B. Epron, C. Bonal, G. Steinhauser, F. Götzfried, Sodium Chloride, Ullmann's Encyclopedia of Industrial Chemistry, Wiley-VCH Verlag GmbH & Co. KGaA: Weinheim, Germany, 2010, https://doi.org/10.1002/14356007.a24_317.pub4.
- [14] E. Aksamija, Der Taylor-Couette Disc Contactor(TCDC), Ein Vereinfachtes Und Optimiertes Design Von Drehscheibenextraktoren, Graz University of Technology, 2014. PhD Thesis.
- [15] E. Aksamija, C. Weinländer, R. Sarzio, M Siebenhofer, The Taylor-Couette disc contactor: a novel apparatus for liquid/liquid extraction, *Sep. Sci. Technol.* 50 (18) (2015) 2844–2852, <https://doi.org/10.1080/01496395.2015.1085406>.
- [16] D. Painer, S. Lux, A. Graftschafter, A. Toth, M Siebenhofer, Isolation of carboxylic acids from biobased feedstock, *Chemie-Ingenieur-Technik* 89 (1) (2017) 161–171, <https://doi.org/10.1002/cite.201600090>.
- [17] G. Rudelstorfer, M. Neubauer, M. Siebenhofer, S. Lux, A Graftschafter, Esterification of acetic acid with methanol and simultaneous product isolation by liquid-liquid extraction in a Taylor-Couette disc contactor, *Chemie Ing. Tech.* 94 (5) (2022) 671–680, <https://doi.org/10.1002/cite.202100184>.
- [18] A. Graftschafter, M Siebenhofer, Design rules for the Taylor-Couette disc contactor, *Chemie-Ingenieur-Technik* 89 (4) (2017) 409–415, <https://doi.org/10.1002/cite.201600142>.
- [19] A. Graftschafter, E. Aksamija, M Siebenhofer, The Taylor-Couette disc contactor, *Chem. Eng. Technol.* 39 (11) (2016) 2087–2095, <https://doi.org/10.1002/ceat.201600191>.
- [20] A.S Mijumdar, Handbook of Industrial Drying, 2014, <https://doi.org/10.1201/b17208.FourthEdition>.
- [21] GESTIS-Database <https://gestis.dguv.de/data?name=011980> (accessed Nov 2, 2022).
- [22] H. Faggion, P.S. Gaschi, M.L. Corazza, L. Cardozo-Filho, L. Igarashi-Mafra, M. R Mafra, NaCl and KCl effect on(vapour + liquid) equilibrium of binary, ternary and quaternary systems involving water, ethanol and glycerol at low pressures, *J. Chem. Thermodyn.* 98 (2016) 95–101, <https://doi.org/10.1016/j.jct.2016.02.026>.
- [23] W.D. Seider, D.R. Lewin, J., .D. Seader, S. Widagdo, R. Gani, K.M Ng, *Product and Process Design Principles: Synthesis, Analysis and Evaluation*, 4 th, Wiley, 2016.
- [24] Luyben, W.L. *Distillation Design and Control Using Aspen™ Simulation*; Luyben, W.L., Ed.; John Wiley & Sons, Inc.: Hoboken, New Jersey, 2013. <https://doi.org/10.1002/9781118510193>.
- [25] D.R Woods, *Rules of Thumb in Engineering Practice*, Wiley-VCH Verlag GmbH & Co. KGaA, 2007.
- [26] R. Turton, J.A. Shaeiwitz, D. Bhattacharyya, W.B Whiting, *Analysis, Synthesis, and Design of Chemical Processes*, 5th ed, Pearson Education Inc., 2018.
- [27] United States Environmental Protection Agency. Defining Hazardous Waste: listed, Characteristic and Mixed Radiological Wastes <https://www.epa.gov/hw/defining-hazardous-waste-listed-characteristic-and-mixed-radiological-wastes#corrosivity> (accessed Apr 13, 2023).
- [28] a H. Hazimah, T.L Ooi, Recovery of glycerol and diglycerol from glycerol pitch recovery of glycerol and diglycerol from glycerol pitch, *J. Oil Palm Res.* 15 (1) (2003) 1–5.
- [29] U.S. Geological Survey. *Mineral Commodity Summaries* 2022; 2022. <https://doi.org/10.3133/mcs2022>.
- [30] A.R. Velez, J.R. Mufari, L.J. Rovetto, Sodium salts solubility in ternary glycerol+water+alcohol mixtures present in purification process of crude glycerol from the biodiesel industry, *Fluid Phase Equilib.* 497 (2019) 55–63, <https://doi.org/10.1016/j.fluid.2019.05.023>.
- [31] A. Rodrigues, J.C. Bordado, R.G.dos Santos, Upgrading the glycerol from biodiesel production as a source of energy carriers and chemicals—a technological review for three chemical pathways, *Energies* 10 (11) (2017) 1817, <https://doi.org/10.3390/en10111817>.
- [32] Intratec. Potassium Sulfate Price <https://www.intratec.us/ch/emical-markets/potassium-sulfate-price>(accessed Apr 13, 2023).
- [33] Waste Business Journal. Waste Market Overview & Outlook 2019 <http://www.was-tebusinessjournal.com/overview.htm> (accessed Apr 13, 2023).
- [34] Thompson, J.; Watson, R.; Galantino, C.; Weiler, C. No End in Sight to US Landfill Cost Increases — Pacific Region to Experience Highest Growth <https://sweepstand.org/no-end-in-sight-to-us-landfill-cost-increases-pacific-region-to-experience-highest-growth/> (accessed Apr 13, 2023).